Electronic Supplementary Material (ESI) for Environmental Science: Water Research & Technology.

Supporting information

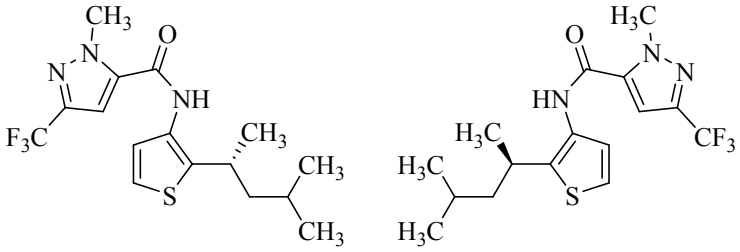

Penthiopyrad

Fig. S1 Chemical structure of penthiopyrad.

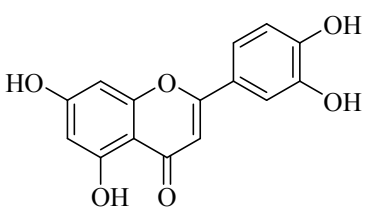

Luteolin

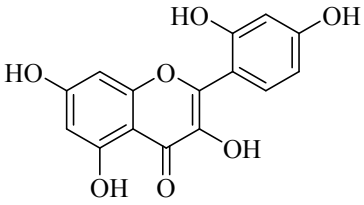

Morin

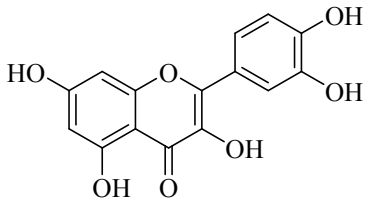

Quercetin

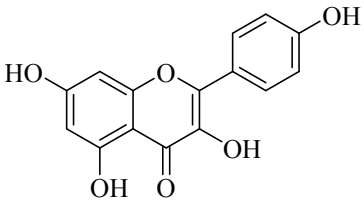

Kaempferol

Fig. S2 Chemical structure of luteolin, morin, quercetin and kaempferol.

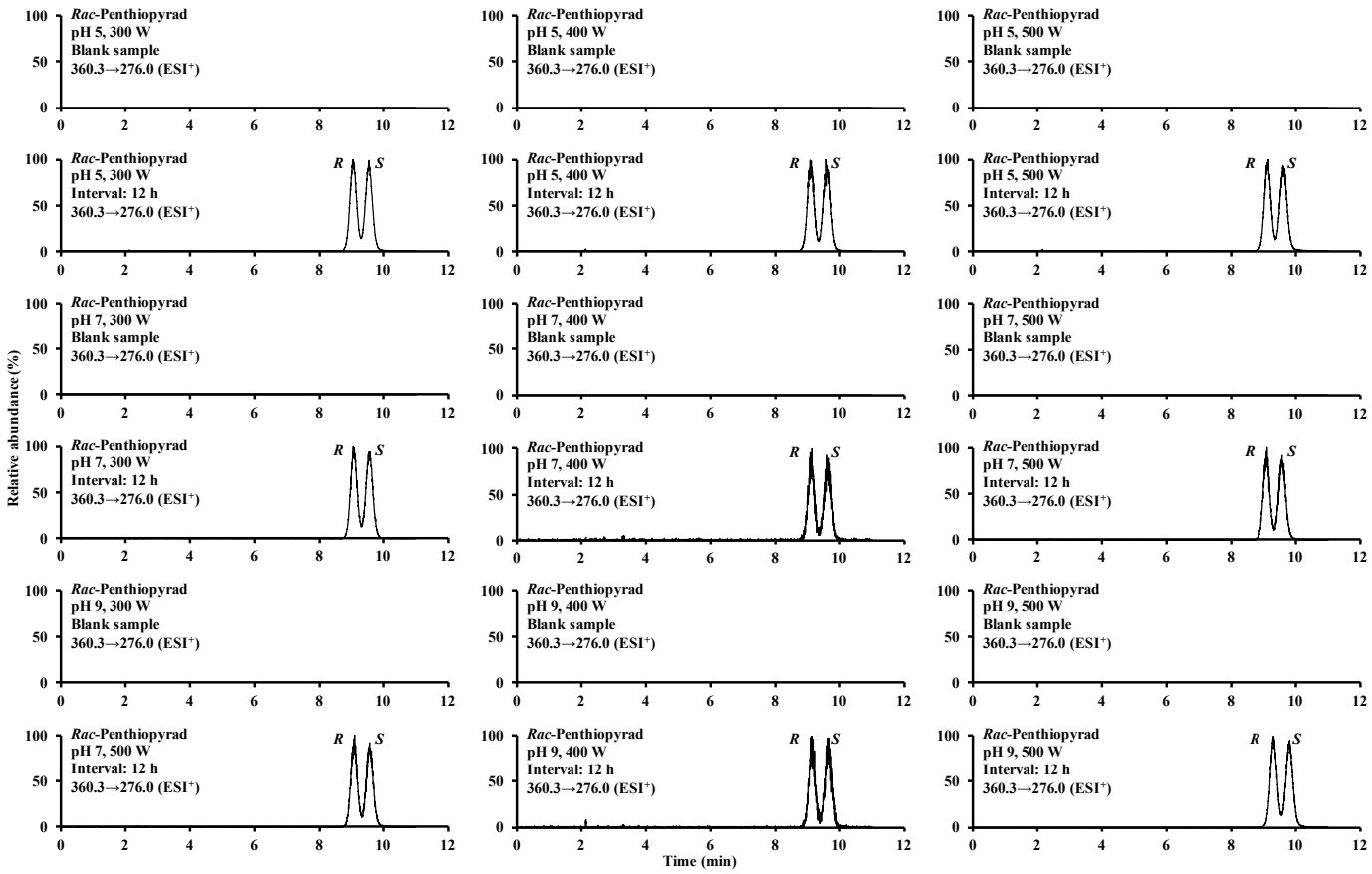

Fig. S3 Typical LC-MS/MS chromatograms of *rac*-penthiopyrad photolyzation in different blank and actual aqueous solutions under three illumination intensities (sampling interval: 12 h).

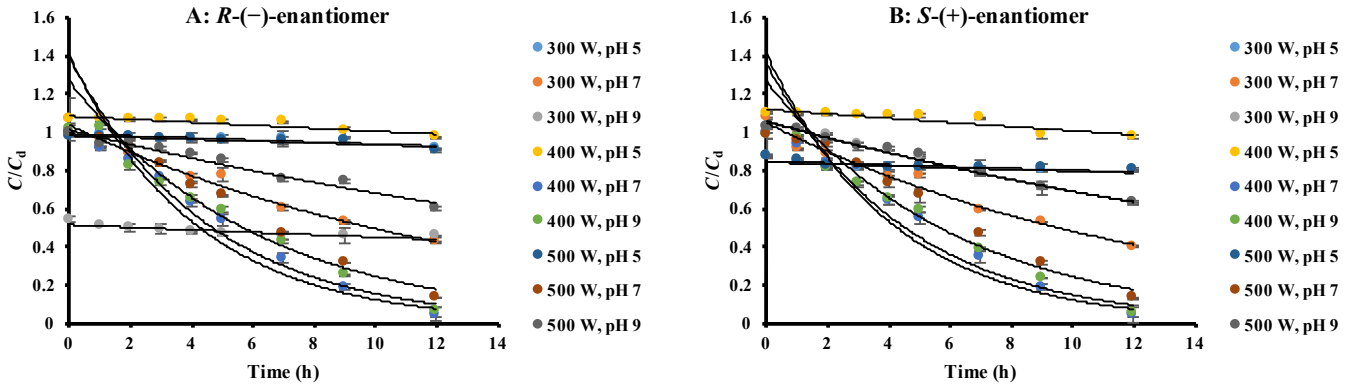

Fig. S4 Photolytic experimental results on the kinetics of *R*-(−)-enantiomer (A) and *S*-(+)-enantiomer (B) of *rac*-penthiopyrad together with curves of pseudo first-order decay fitted to the data by nonlinear regression obtained for different buffer solutions under different illumination intensities (Note that, for the majority of the experimental points, error bars are so small that they are not visible in the figure, *n* = 3).

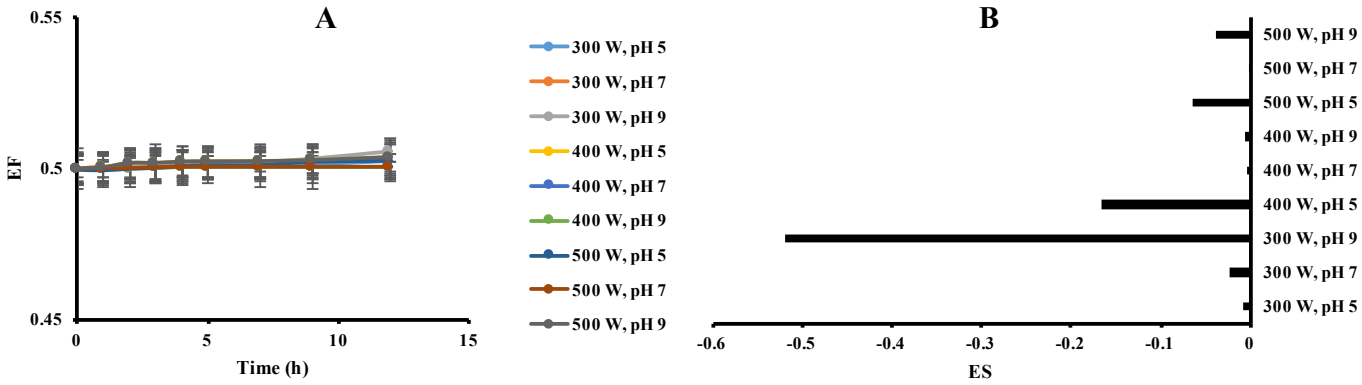

Fig. S5 EF-time curves (A) and ES values (B) of *rac*-penthiopyrad photolyzation in different buffer solutions under different illumination intensities (*n* = 3).

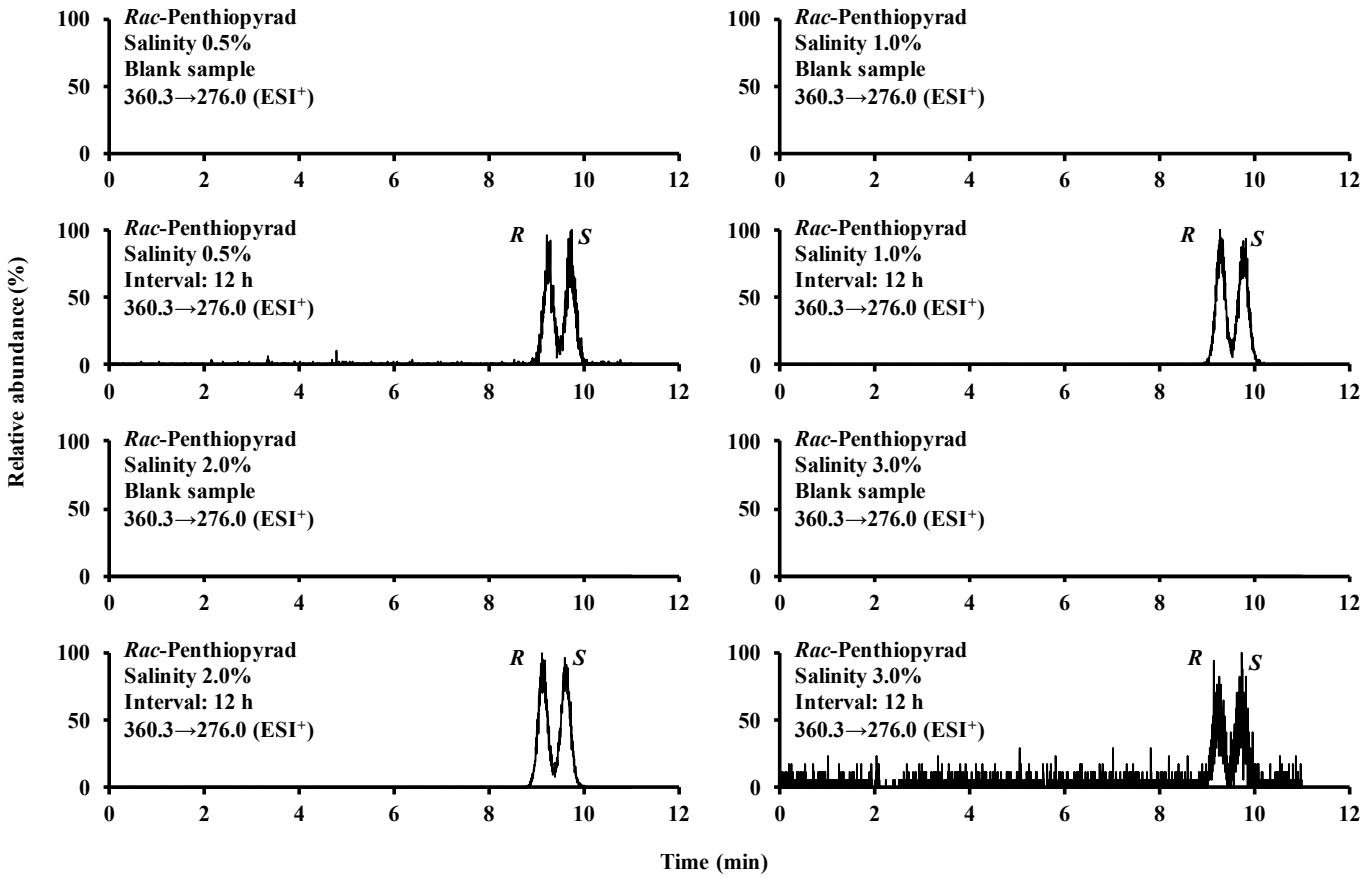

Fig. S6 Typical LC-MS/MS chromatograms of *rac*-penthiopyrad photolyzation in different blank and actual pH 7 aqueous solution with different salinities under illumination intensity 400 W (sampling interval: 12 h).

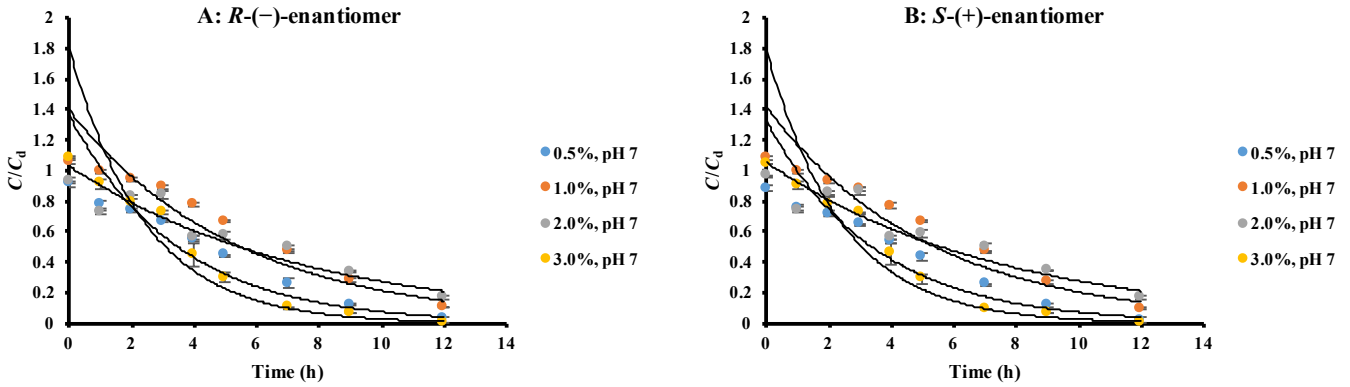

Fig. S7 Photolytic experimental results on the kinetics of *R*-(−)-enantiomer (A) and *S*-(+)-enantiomer (B) of *rac*-penthiopyrad together with curves of pseudo first-order decay fitted to the data by nonlinear regression obtained for pH 7 buffer solution with different salinities (Note that, for the majority of the experimental points, error bars are so small that they are not visible in the figure, *n* = 3).

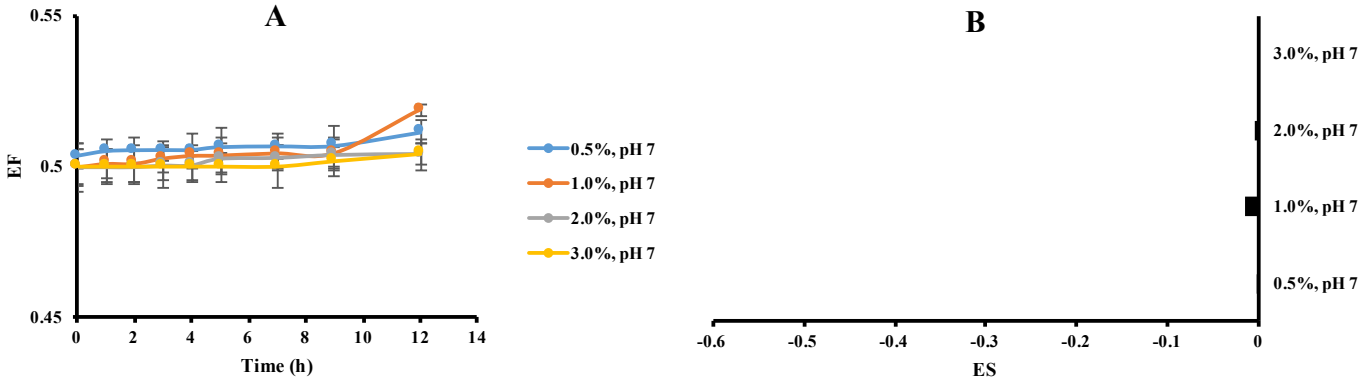

Fig. S8 EF-time curves (A) and ES values (B) of *rac*-penthiopyrad photolyzation in pH 7 buffer solution with different salinities (*n* = 3).

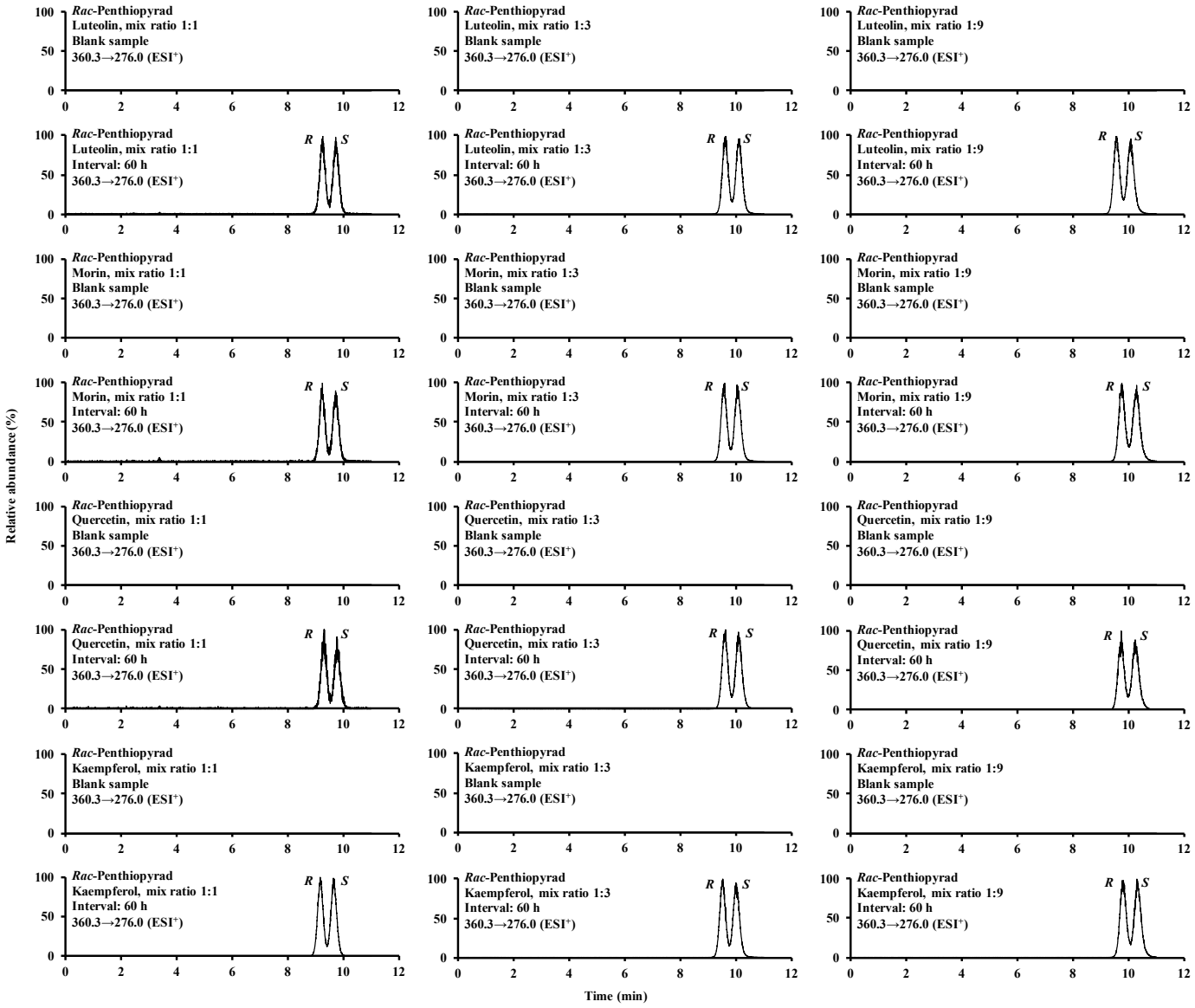

Fig. S9 Typical LC-MS/MS chromatograms of *rac*-penthiopyrad photolyzation in different blank and actual pH 7 aqueous solution with different mix ratios of penthiopyrad and flavonoid under illumination intensity 400 W (sampling interval: 60 h).

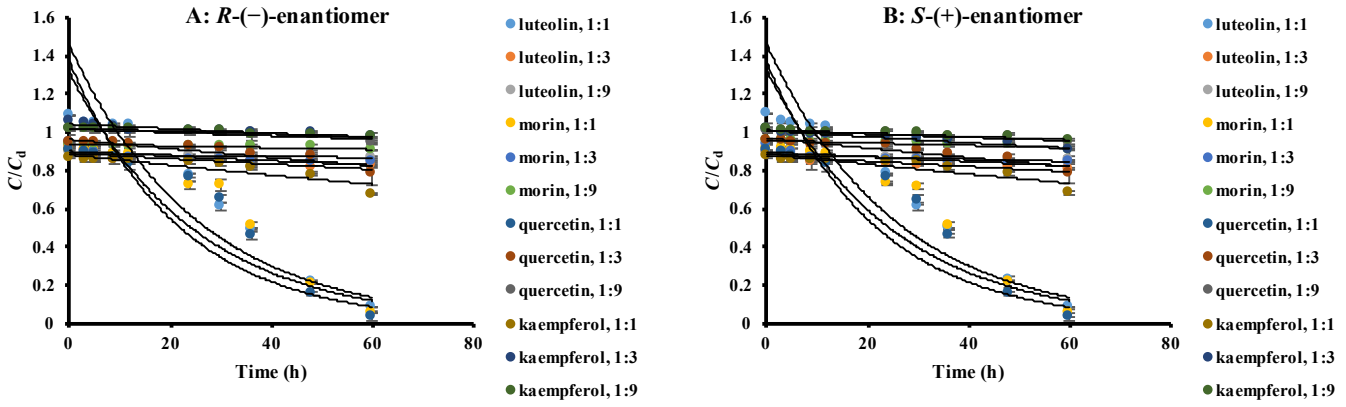

Fig. S10 Photolytic experimental results on the kinetics of *R*-(−)-enantiomer (A) and *S*-(+)-enantiomer (B) of *rac*-penthiopyrad together with curves of pseudo first-order decay fitted to the data by nonlinear regression obtained for pH 7 buffer solution with different mix ratios of penthiopyrad and flavonoid (Note that, for the majority of the experimental points, error bars are so small that they are not visible in the figure, *n* = 3).

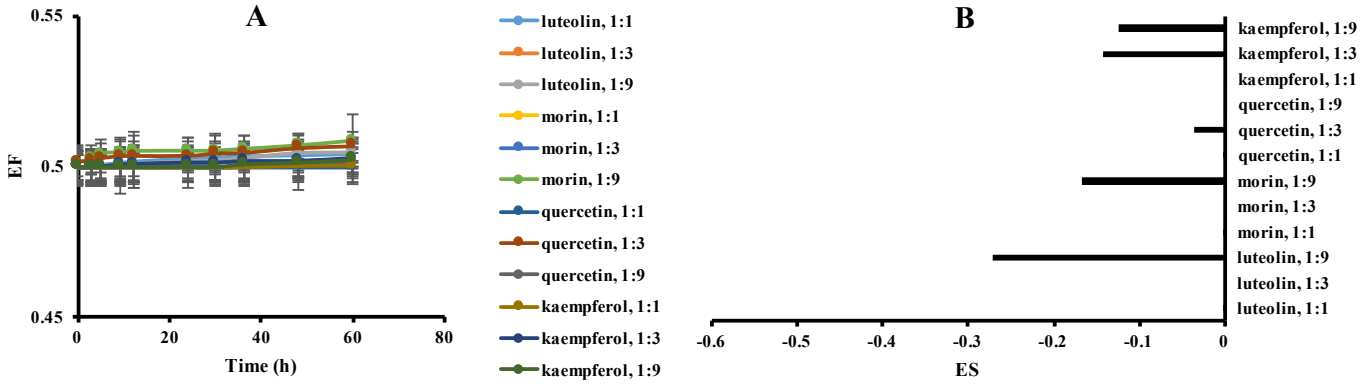

Fig. S11 EF-time curves (A) and ES values (B) of *rac*-penthiopyrad photolyzation in pH 7 buffer solution with different mix ratios of penthiopyrad and flavonoid (*n* = 3).

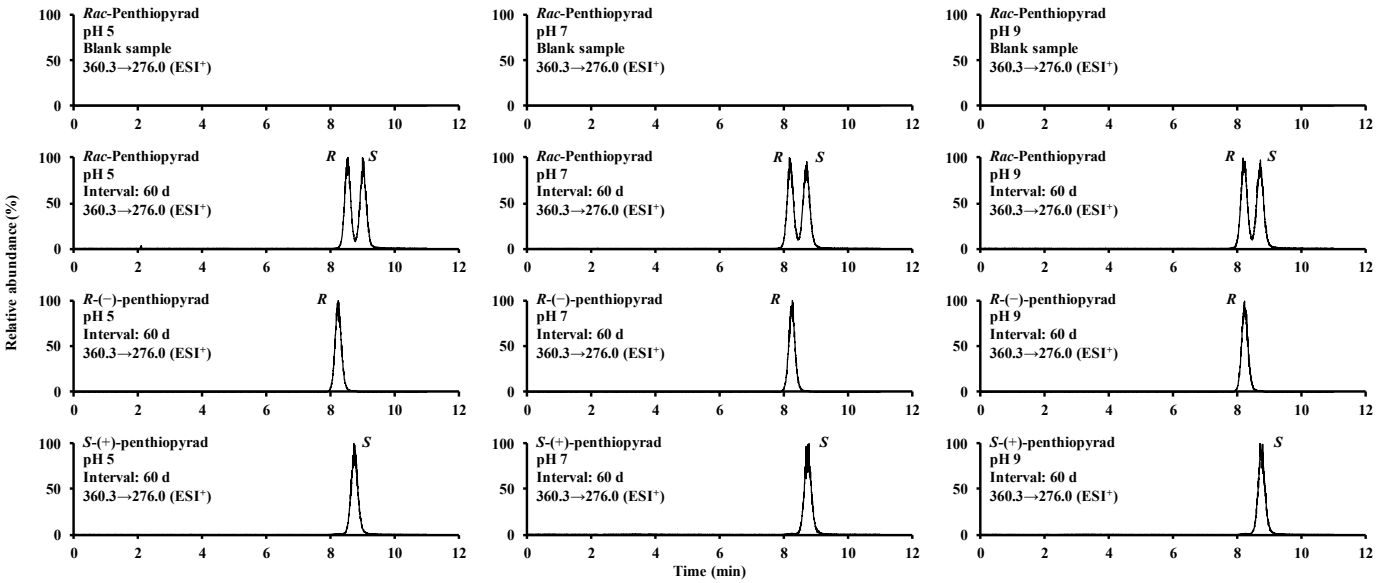

Fig. S12 Typical LC-MS/MS chromatograms of racemic and enantiopure penthiopyrad hydrolysis in different control and actual aqueous solutions at 25 °C (sampling interval: 60 d).

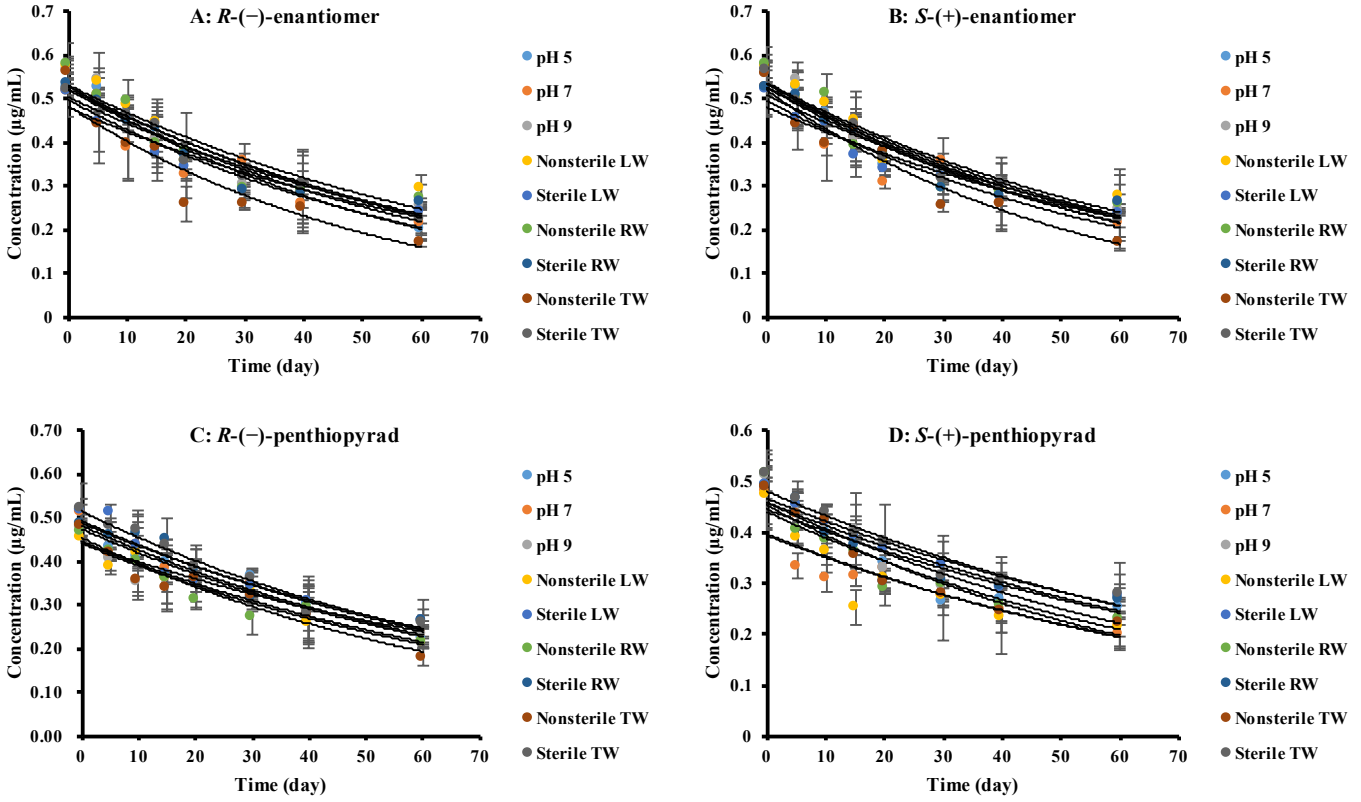

Fig. S13 Hydrolytic dynamics curves of *R*-(−)-enantiomer (A) and *S*-(+)-enantiomer (B) of *rac*-penthiopyrad, and enantiopure *R*-(−)-penthiopyrad (C) and *S*-(+)-penthiopyrad (D) in different aqueous solutions incubated at 25 °C; LW: lake water, RW: rain water, TW: tap water (Note that, for the majority of the experimental points, error bars are so small that they are not visible in the figure, $n = 3$).

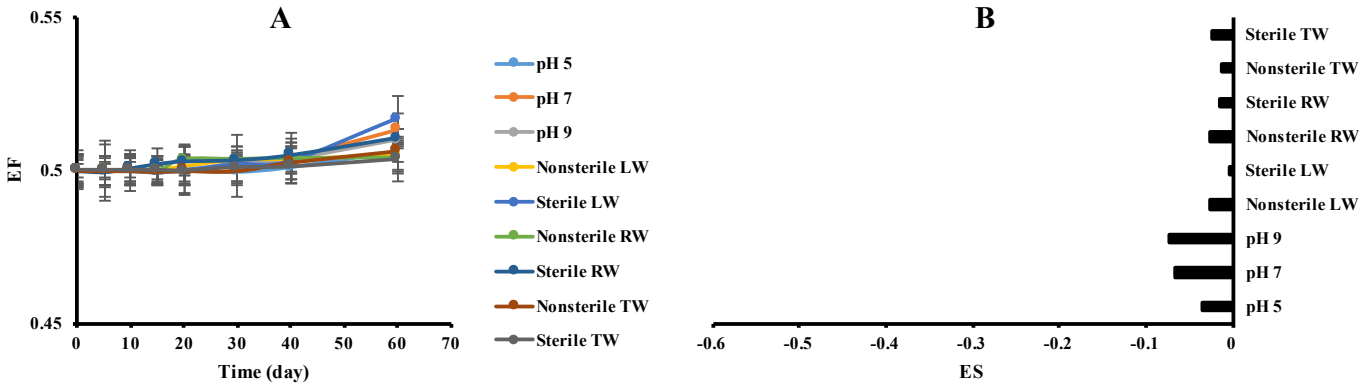

Fig. S14 EF-time curves (A) and ES values (B) of *rac*-penthiopyrad hydrolyzation in different aqueous solutions incubated at 25 °C; LW: lake water, RW: rain water, TW: tap water ($n = 3$).

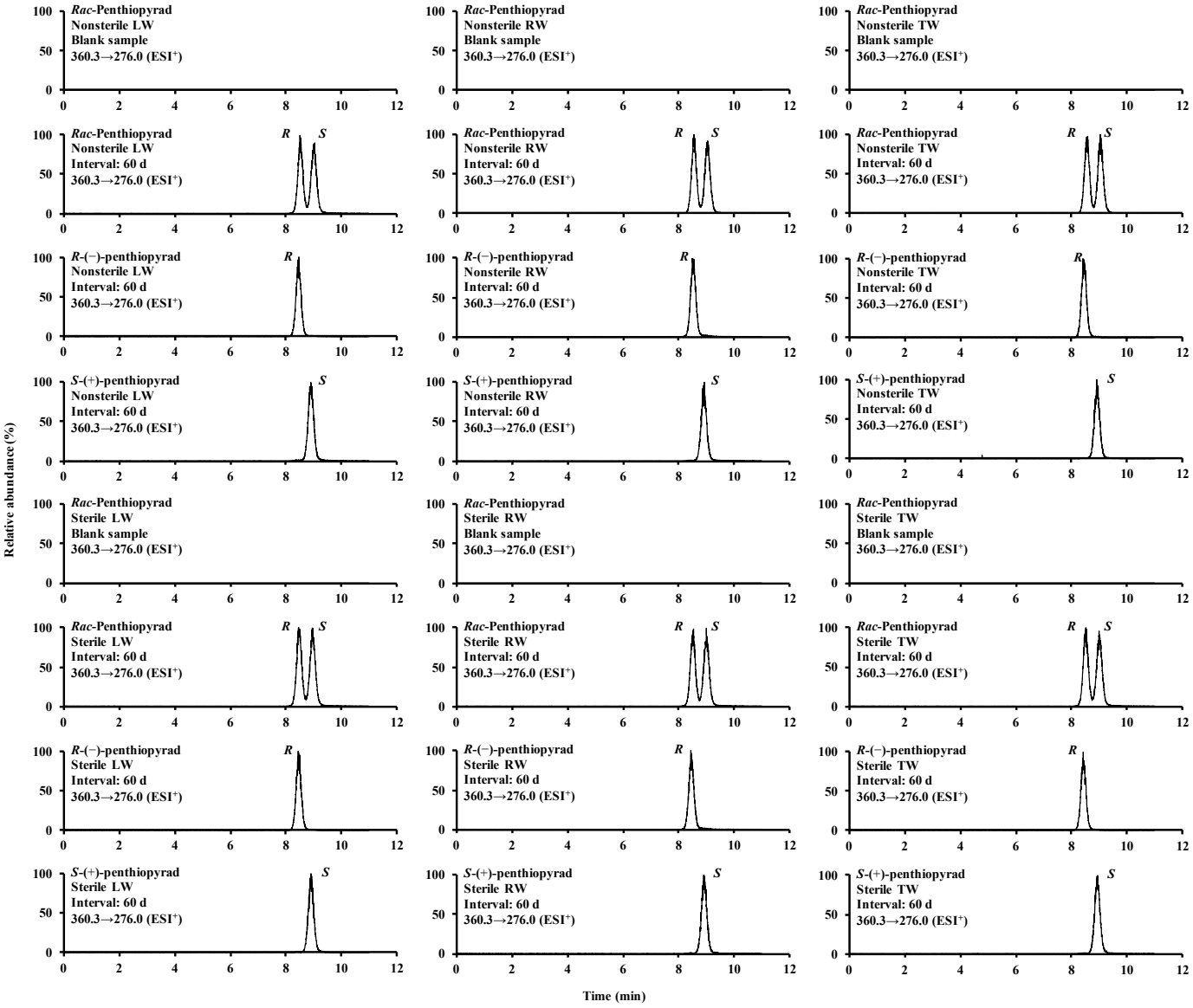

Fig. S15 Typical LC-MS/MS chromatograms of racemic and enantiopure penthiopyrad hydrolysis in different control and actual sterile/nonsterile natural water matrices at 25 °C; LW: lake water, RW: rain water, TW: tap water (sampling interval: 60 d).

Table S1 LC-MS/MS parameters for detection of penthiopyrad enantiomers in water

Parameter	Data
LC conditions (UFLC DGU-20A LC system, Shimadzu Corporation, Kyoto, Japan)	
Column	Superchiral S-OD chiral column (150 × 4.6 mm i.d.; particle size, 5 μm; Shanghai Chiralway Biotech Co., Ltd., Shanghai, China)
Mobile phase	Acetonitrile (0.1% formic acid):0.1% formic acid aqueous solution = 50:50 (*v*/*v*)
Flow rate	1.0 mL/min
Injection volume	3 μL
Column temperature	30 °C
Retention time	11 min
MS conditions (Sciex 4000 Q-Trap triple quadrupole MS system, Applied Biosystems, Foster City, USA)	
Gas source	Nitrogen (purity, 99.999%)
Pressure of ion source gas 1 and 2	65 psi
Ion spray voltage	5500 V
Ion source temperature	600 °C
Electron ionization mode	Positive (ESI^+)
Monitoring mode	Multiple reaction monitoring (MRM)
m/*z*	360.3→256.0 (confirmation), 360.3→276.0 (quantification)
Declustering potential (DP)	103.5 V
Entrance potential (EP)	10.0 V
Collision energy (CE)	28.7 (daughter ion 256.0), 18.4 (daughter ion 276.0)
Collision cell exit potential (CXP)	15.7 (daughter ion 256.0), 25.9 (daughter ion 276.0)

Table S2 Linearity, determination coefficient (R^2), matrix effect (ME), limit of detection (LOD) and quantitation (LOQ) of penthiopyrad enantiomers in solvent and water samples

Analyte	Solvent/matrix	Regression equation	R^2	ME	LOD (μg/mL)	LOQ (μg/mL)
R-(−)-enantiomer	Acetonitrile	$y = 322344x + 8899$	0.9971	/	/	/
	Water	$y = 313035x + 4085$	0.9988	0.97	0.003	0.01
S-(+)-enantiomer	Acetonitrile	$y = 320779x + 9008$	0.9968	/	/	/
	Water	$y = 312050x + 3866$	0.9989	0.97	0.003	0.01

ME = the slope of solvent standard calibration curve / the slope of matrix-matched standard calibration curve.

LOD was calculated using a signal-to-noise ratio (*S*/*N*) of 3 and LOQ was defined as the lowest spiked concentration.